PREPRINT UCRL-77790

CONF-760513--8

Lawrence Livermore Laboratory

Focusing Lenses for the 20-Beam Fusion Laser, SHIVA

William C. O'Neal

May 18, 1976

This paper was prepared for submission to the 1976 IEEE/OSA Conference on Laser and Electro-Optical Systems on May 25-27, 1976 in San Diego, California.

FOCUSING LENSES FOR THE 20-BEAM FUSION LASER, SHIVA

William C. O'Neal L-541
Lawrence Livermore Laboratory
Livermore, California 94550
(415) 447-1100 X-4316

ABSTRACT

The focus lens design for the 20-beam SHIVA laser fusion facility involves considerations of uniform and normal pellet illumination. The resulting requirements dictate tailored beam intensity profiles and vacuum-loaded thin lenses.

FOCUSING LENSES FOR THE 20-BEAM FUSION LASER, SHIVA*

William C. O'Neal
Lawrence Livermore Laboratory
P. O. Box 808 (L-541)
Livermore, California 94550
(415) 447-1100 X-4316

SUMMARY

The SHIVA HIGH ENERGY LASER FACILITY now under construction at Lawrence Livermore Laboratory is a 20 arm, 1.06 μM Nd-glass laser system that can focus 20-30 TW of power nearly uniformly on a 300-1500 μM diameter deuterium-tritium laser fusion pellet. The facility will be in operation in 1977, and should produce significant thermonuclear burn (fusion energy output = 1% light energy input). Figure 1 shows the SHIVA target chamber with lenses. Figure 2 shows the entire high energy laser facility.

FOCUSING REQUIREMENTS

The illumination uniformity requirements for high final compression of the imploding pellet are that, during the first 10% power deposition of the pulse, the variation of the intensity over the target surface must be less than ± 10% to initiate a spherically smooth implosion. During the rest of the 100 picosecond pulse, optical intensity variations of as much as 50% will be smoothed out by electron conduction in the absorbing plasma. In order to achieve the illumination smoothness and and the 10 μRad pointing and 7 μM focusing accuracy, the static quality of the optical chain including focus lenses, must be less than 1/2 wave, 1 σ rms at 1.06 μM.

Computer and hand calculations show that if the rms sum of the specified allowable peak wavefront distortions of all the optical elements that refract or reflect the beam is < 1/2 wave, with ? sinusoidal 'ase cycles across the beam,

*Work performed under the auspices of the U.S. Energy Research & Development Administration under contract No. W-7405-Eng-48.

the illumination variation across the near-field focused beam is within ± 5% of a quadratic intensity profile. (The target surface is about 1.5 mm before the focal plane of the lens.) A simple hand calculation of a local intensity variation from a local phase distortion can be made assuming geometrical optics. If a sinusoidal phase error defocuses a portion of the beam, the "lens effect" will decrease the focal angle of the local bundle of rays, reducing the near field intensity on the target. The approximate intensity reduction, I, is given by:

$$I \approx 1 \Big/ \left[1 + \frac{\pi (f^{\#})^2 P}{(d/D)^2 \Delta Z} \right]^2$$

f# = f/number of lens

D = diameter of lens

P = peak to peak phase error

d = "diameter" of local phase "bump" = half period of sinusoidal phase disturbance

ΔZ = distance from target surface to focal plane.

Figure 3 shows the geometrical approximation for this model. Figure 4 shows I as a function of peak to peak phase distortion, diameter of aberrated region, and target size. For SHIVA, a small sized local error is as important as a large area error since either can initiate a non-symmetrical implosion which will degrade the final density-temperature level of the compressed pellet.

ERROR BUDGET

The rms aberrations of the laser chain and turning mirrors approach 1/2 wave, leaving little in the optical error budget[1] for the final focus lens. The lens specification allows a peak to peak phase distortion of no more than 1/10 wave at 1.06 μM with a maximum slope error of 1/30 wave/cm, which causes less than a 3% intensity variation for a 1 mm pellet 1.5 mm in front of the focal plane. The error budget allows a total of ± 5% intensity variation on target[1] for one beam. An aberration corrector is being developed in case whole chain phase distortions are excessive.

INTENSITY MAPPING BY THE FOCUS LENS

A beam intensity profile is changed in shape when focused through a lens onto a sector of the target surface.[2] Also, since the target plasma refracts out a portion of the light depending on the angle of incidence, via inverse bremsstrahlung or other processes[3], the intensity profile is further changed, since the angle of incidence of each ray is not constant for a beam focused at planes other than target center. Figure 5 shows a beam focused at a plane beyond the target. When 20 beams are icosahedrally located and focused, as shown in Figure 6, the overlapped spots sum to a high illumination uniformity, according to the LLL LUXCON code, if the proper intensity profile is provided.

INTENSITY PROFILE FUNCTIONS

The expressions for the intensity profiles[4] are:

$f = f_o[1-(r/r_p)^2]$, intensity of quadratic portion of profile

$g = A(r_c-r)^B$, intensity of power fillet portion of profile

r_c = cutoff radius of power fillet for $I=0$

$R = r_1/r_c$, match point of the two portions of the curve

$I = f_1/f_o$, fractional intensity at match point

$r_p = Rr_c(1-I)^{-1/2}$, r for zero intensity of quadratic

$B = 2\,\frac{(1-R)(1-I)}{RI}$, fillet power

$A = (f_o/r_c^B)\,[I/(1-R^B]$, fillet scale

When B > 1 or when I < 1-R/1-(R/2), the fillet meets the cutoff edge with zero slope. When B < 1, the fillet slope is infinite at cutoff.

The LUXCON target profile functions used in this report are:

$$I = I_o[1-r/r_p]^2, \quad r_p = .817, \text{ quadratic portion}$$

$$R = .63, \; I = .405, \text{ match point}$$

$$I = 2.25(1-r)^{1.7257}, \text{ power fillet portion}$$

The beam profile functions are:

$$I = I_o[1-r/r_p]^2, \quad r_p = .949, \text{ quadratic portion}$$

$$R = .9, \; I = .1, \text{ match point}$$

$$I = 10(1-r)^2, \text{ power fillet portion}$$

The above values and profile calculations are conveniently calculated with the HP 65 using Trenholme's program chip.

There are other possible absorbing processes which may affect illumination uniformity on the imploding surface, but we have decided to evaluate the design of the illumination system using inverse bremsstrahlung alone.[3] The absorption of light by the plasma is given by:

$$\overline{A} = 1-e^{-2P\cos^5(\theta-\beta)}$$

where

$\overline{A}$ = plasma absorbtivity

P = optical thickness of plasma at normal incidence

θ = target wrap angle

β = ray angle

$\theta-\beta$ = angle of incidence

$e^{-2P\cos^5(\theta-\beta)}$ = plasma reflectivity

LENS-TARGET INTENSITY MAPPING

By definition, Intensity = Power ÷ Area. If a set of equal spaced beam rays is focused beyond the target, the relative spacing and thus the annular area between the rays is different on the target surface. Since power is invariant from beam to target,

$$\frac{I_B/P_B}{I_T/P_T} = \frac{A_T}{A_B}$$

and

$$\frac{I_T}{I_B} = \frac{A_B}{A_T} \equiv L,$$

L is the lens/target mapping function.

As shown on Figure 5, the beam area is:

$$A_B = \frac{\pi\ (r_2^2 - r_1^2)}{\pi\ r_o^2} = r_2^2 - r_1^2,\ (r_o = 1) \tag{1}$$

The target area is given by:

$$A_T = \int_{\theta_1}^{\theta_2} 2\pi r_t^2 \sin\theta d\theta = 2\pi r_t^2\ (\cos\theta_2 - \cos\theta_1)$$

setting $\theta_1 = \theta_o$ and $\theta_2 = 0^0$ gives the total area, $2\pi r_t^2\ (1-\cos\theta_o)$, and the normalized target area is:

$$A_T = \frac{2\pi r_t^2\ (\cos\theta_2 - \cos\theta_1)}{2\pi r_t^2\ (1-\cos\theta_o)} = \frac{\cos\theta_2 - \cos\theta_1}{1-\cos\theta_o} \tag{2}$$

The mapping function is given by:

$$L = \frac{A_B}{A_T} = \frac{(r_2^2 - r_1^2)\ (\cos\theta_2 - \cos\theta_1)}{1-\cos\theta_o} \tag{3}$$

From Figure 4 and the law of sines,

$$\beta = \sin^{-1}\left(\frac{Q}{r_t}\sin\theta\right) + \theta, \tag{4}$$

$$\frac{Q}{r_t} = \frac{\sin(\theta-\beta)}{\sin\theta}.$$

For an aplanatic lens,

$r = f \sin \beta$

f = focal length.

For other lens designs, and for aberrated beams, $\beta(r)$ is determined by a ray trace.

TOTAL MAPPING FUNCTION

The lens/target/plasma mapping function is given by:

$$M = LB$$

$$B = 1-e^{-2P\cos^5(\theta-\beta)} \Big/ 1-e^{-2P}, \text{ (normalized absorbtivity)}$$

$$M = \frac{(r_2^2-r_1^2)\ (\cos\theta_2-\cos\theta_1)\ (1-e^{-2P\cos^5[\theta-\beta]})}{(1-\cos\theta_o)\ (1-e^{-2P})} \tag{5}$$

Equations 2 through 5 have been programmed individually and in combinations for the HP 65. Using these programs, and analytic and numerical integration, tables such as Table 1 can be generated to give mapping factors at various r/r_o and θ/θ_o. When a given point on an intensity profile is multiplied or divided by the calculated mapping factor, a new point is found, and a new intensity profile is developed, as shown in Figure 7. The new profile is then best fitted to a power-filleted quadratic by successive trials.

ABSORPTION EFFICIENCY

The fraction of the beam energy absorbed in the target plasma is:

$$\varepsilon_A = \frac{\int_0^r \int_0^\theta \int_0^A I_{(r)} \bar{A}\, dr\, d\theta\, dA}{\int_0^r \int_0^A I_{(r)}\, dr\, dA} = \frac{\text{absorbed power}}{\text{incident power}}$$

The numerical integration of this from Table 1 (for a .8/.2 laser profile) gives an absorption of 53% of the beam. Since this fraction would be 63% if the illumination angle of incidence was zero for all rays, the illumination efficiency, ε_I, is .53/.63 = 84%.

The overall mapping function applied to a good fill factor beam (R=.9, I=.1) gives a softer-tailed profile (R=.63, I=.405) wrapped on the target. Fortunately, LUXCON indicates the target requires soft-tailed profiles for high uniformity. However, soft-tailed profiles must be well wrapped through the target, causing more anormality and resulting loss in power through inverse bremsstrahlung. Experimental variation of these parameters on SHIVA will determine the optimum illumination geometry.

The F/1.62 aplanatic lens has a small effect on mapping compared to inverse bremsstrahlung, and should be satisfactory for the SHIVA baseline system.

F/NUMBER OF LENS

An examination of Table 1 shows that the outer rays of the focused beam undergo a plasma absorption $\bar{A}$, of 0.299, compared to the central ray absorption of 0.632, demonstrating the additional loss by inverse bremsstrahlung if the ray angles are not normal to the surface of the pellet. The outer rays of low f-number lenses are more nearly normal to the pellet surface when the pellet center is located ahead of the lens focal plane. Therefore lower f-numbers provide more absorption of light. For SHIVA, f/1.6 is the lowest f-number for a group of 20 lenses which can be assembled, and held with room for adjustment in an icosahedral array around the pellet.

LENS THICKNESS

The total thickness of all high-power optical elements in the chain must be kept to a minimum to reduce self-focusing[6] of the beam. The B integral[7] of an optical material in a high intensity beam is a measure of the self focusing effect. It is given by:

$$B \simeq .02 \int_0^z I dz \quad \text{for BK7 glass, where:}$$

I = intensity, GW/cm^2

n_2 = non-linear index $\simeq 1.24 \times 10^{-13}$ esu

z = thickness of element

Using a minimum thickness focus lens as a vacuum barrier reduces the thickness of optical material in the beam. However, surface cracks from self-focusing or ghost focusing damage can cause a sudden fracture of the lens or window, which may be hazardous to personnel and nearby equipment. Since laser performance is improved by minimizing glass thickness, a safe lower limit on thickness must be established.

The vacuum side of the lens is in tensile stress, the exact value of which can be determined by a finite element code (for lenses) or, for a plane window, the maximum stress (at the center, simply supported edge) is given by:

$$\sigma = \frac{3W(3m+1)}{8\pi m t^2}$$

W = load, pressure x area

m = 1/Poisson ratio

t = thickness

Figure 8 shows the stress and deflection of a window as a function of the D/T ratio.

For a given tensile stress, there is a surface crack depth, "a", which will cause sudden fracture of the lens or window:

$$a = \frac{Q}{1.21\pi} \left(\frac{K_{1C}}{\sigma} \right)^2$$

Q = crack geometry and stress level parameter. (Q=1 for low stress and long crack)

K_{1C} = plain strain fracture toughness, $KSI \cdot in^{1/2}$ (1000 for glasses in vacuum and 500 for glasses in air)

σ = maximum surface stress, psi

Figure 8 shows critical (massive fracture) crack depth vs d/t ratio for windows. The equivalent d/t for a lens can be determined by dividing the diameter by the thickness at $r/r_0 \approx 0.4$.

For example, the SHIVA focus lens has an equivalent d/t of ∿ 12.5. From Figure 1, the stress is ∿ 700 psi. From Figure 8, the critical crack depth is 14 mm. Observed single shot cracks are no more than 2-3 mm deep[8], which gives a safety factor of ∿ 3 on crack depth. Since repeated shots can cause further damage at the crack, an inspection of thin vacuum barrier optics should be done after each high power shot.

LENS MATERIAL

The considerations for lens material are the cost of high optical quality material having a low n_2 (non-linear index of refraction) and the dollar value of the increase in focusable laser power available due to the lower n_2. For SHIVA, the tradeoff of figure of merit, cost and quality indicated that BK7 was the best choice over fused silica, FK51 and FK5. The figure of merit for a lens is given by:

$$F.M. = n(n-1)/n_2$$

n = index of refraction

n_2 = non-linear index of refraction

The lens specification (Appendix) lists the material requirements.

POTENTIAL DAMAGE FROM INTERNAL GHOST IMAGES

Progressive internal lens damage has commonly occurred in the central region of high-power laser-fusion focusing lenses.[2,9] The solution has been to bore 2-5 mm holes and cut circular saw slots to reflect the ghost rays before they focus to the internal damage level. Avoiding the resulting shadow on the pellet caused by such irregularities will enable SHIVA to achieve the < 10% initial intensity uniformity required for highest density-temperature levels in the compressed pellet. To this end, the focus lens has been designed as an F/1.6 doublet with very low reflectivity (0.1% @ 15°) AR coatings. Analysis of various bending geometries on the ghost program[10], an LLL intensity-ray trace code, shows the ghost caustic intensity in the design selected to be no more than the incoming beam intensity. Figure 9 shows the reflectivity vs angle of incidence required on all surfaces to attain the low caustic intensity.

SHIVA F/1.6 FOCUS LENS FINAL DESIGN

The final design of the SHIVA F/1.6 focus lens, shown in Figure 10, to be used for near field uniform illumination has the following characteristics:

1) High Uniformity. The lens aberrations will cause less than a 3% variation of the illumination profile for a 1000 μm diameter target, and less than 5% for a 30[illegible] μm diameter target.

2) Low Ghost Focus Intensity. The coated lens is designed for ghost focus intensity less than the intensity of the incoming beam for laser rays or target reflected rays. Therefore, no hole is required in the lens.

3) Vacuum Deflection. A vacuum deflection test on a lens of the same F# and same d/t ratio, but 2/3 the diameter showed root mean squared spherical aberration of $\lambda/40$ at 1.06 μm. Based on these results, the SHIVA lens $\lambda/10$ figure will not have to be corrected for vacuum deflection, but will be tested in the deflected and undeflected conditions.

4) Separable Elements. The first element is an F/2.5 lens with a 736 mm focal length designed with zero spherical aberration and $\lambda/14$ coma (for 0.1 mrad of tilt or field). To lower the F# to F/1.6, the second element is added. It is designed with zero spherical aberration for an F/2.5 incoming beam (with no aspheric surfaces). Either lens can be tested by itself, thus facilitating more economical fabrication and interchangeability. The aspheric coefficients for element 1 were determined using the ACCOS V optical design code.

5) Second Element All Spherical. The second surface of the second element can be refinished and recoated (for $1000-$1500, an affordable but expensive outlay) at a frequency depending on the power output and composition of targets, and the effectiveness of blast shields now being developed. The second element protects the vacuum-stressed first element from target debris and radiation.[11]

6) Error Analysis. The results of a tolerance analysis of the F/1.6 doublet given in Table 2 were obtained with the ACCOS V code.

7) Specification. Appendix 1 is the specification for the lens as it appears on LLL Drawing AAA 76-104839.

ACKNOWLEDGEMENTS

The author wishes to acknowledge the invaluable guidance of H. Ahlstrom, E. Bliss, S. Ekstrom, J. Emmett, T. J. Gilmartin, A. Glass, J. Glaze, R. O. Godwin, E. Goodwin, W. Hagen, J. F. Holzrichter, J. Hunt, E. R. McClure, J. Sonderman, J. Trenholme, and P. Wallerstein

REFERENCES

(1) T. J. Gilmartin, UCRL-50021-74, Laser Program Annual Report - 1974, p. 88.

(2) C. E. Thomas, Applied Optics, June 1975, Vol. 6, p. 1267.

(3) J. W. Shearer, UCID-15745, p. 19.

(4) J. Trenholme, Laser Program Annual Report - 1975.

(5) J. Trenholme, UCRL-50021-74, p. 227.

(6) V. I. Bespalov and V. I. Talanov, JETP Lett. 3, 307 (1966).

(7) E. S. Bliss, D. R. Speck, J. F. Holzrichter, J. H. Erkkila, and A. J. Glass, Appl. Phys. Lett. 25, 448 (1974).

(8) W. D. Fountain, LLL, Private Communication.

(9) J. deMetz, Applied Optics 10, 1609 (1971).

(10) J. Trenholme, E. Goodwin, LLL Internal Reports TDA-75-125, TDA-75-183.

(11) W. C. O'Neal, UCRL 77231.

r/r_0	A_B Rel. Beam Area	β Ray Angle	$I_{(r)}$ .8/.2	θ Target Angle	θ-β	A_T Target Area	L $\left(\frac{A_B}{A_T}\right)$	I(θ) (I(r)M)	B $\left(\frac{A}{1-e^{-2F}}\right)$	M (LB)	P_0 Incid. Power $(I(r)A_T L)$	P_A Abs. Power $(P_0 A)$	$\overline{A}$ $1-e^{-2P\cos}$[illegible]	[illegible] Abs. Pow.	[illegible]
1.0		17.178		55	37.822										1
.95	.19	16.29	.0125	51.91	35.6[illegible]	.196	.94	.0056	.473	.445	.0023	.00069	.299	.0011	.94
.90		15.415		48.91	33.50										.89
.85	.17	14.54	.1125	45.96	31.42	.173	.954	.062	.576	.560	.0186	.0068	.364	.0107	.84
.80		13.666	.2	43.04	29.36										.78
.75	.15	12.8	.297	40.19	27.39	.150	.97	.193	.671	.651	.043	.0163	.424	.029	.73
.70		11.93		37.35	25.42										.68
.65	.13	11.07	.472	34.56	23.50	.131	.963	.343	.755	.727	.0595	.0284	.477	.045	.63
.60		10.206		31.72	21.59										.58
.55	.11	9.35	.622	29.06	19.71	.107	.997	.513	.827	.825	.0664	.0347	.523	.055	.53
.50		8.49		26.34	17.85										.48
.45	.09	7.637	.747	23.65	16.02	.088	.992	.657	.886	.800	.0652	.0365	.560	.058	.43
.40		6.783		20.93	14.20										.38
.35	.07	5.933	.847	18.33	12.39	.0682	.996	.786	.952	.928	.0575	.0339	.589	.054	.33
.30		5.082		15.68	10.60										.29
.25	.05	4.234	.922	13.05	8.82	.0485	1	.890	.965	.965	.0447	.0273	.610	.033	.24
.20		3.386		10.43	7.04										.19
.15	.03	2.539	.972	7.82	5.278	.0291	1	.960	.980	.988	.0293	.0177	.624	.028	.14
.1		1.6924		5.208	3.516										.095
.05	.01	.8451	.997	2.605	1.757	0097	1	.996	.999	.999	.0097	.0051	.631	.0093	.047
0	0	0	0	0	0	0	1	1	1	1			.632		0
											Total .3962	Total .2104		Total .3323	

Table 1

55° Mapping, F/1.6

Table 2

Variable	Error	Aberration @ 1.06 µm	Near Field Illumination Variation	
Spacing	± 0.5 mm	λ/17 S.A.		
Thickness of Second Element	- 2 mm	λ/17 S.A.		
Decenter Second Element	± 1 mm	λ/20 coma		
Tilt Second Element	1.7 mrad	λ/25 coma + astig.		
Vacuum Deflection	1 atmos.	λ/30 S.A.		
Total (Arith) Dimensional Error		λ/4, 1 cycle	300 µm target,	3%
			1000 µm target,	1.2%
Lens Figuring Error	Wavefront Distortion	λ/10, 2 cycles	300 µm target,	5%
		λ/24/cm slope error	1000 µm target,	2%
Total All Errors, rms		λ/7, 2 cycles	300 µm target,	8%
			1000 µm target,	3%

FIG. 1

SHIVA TARGET CHAMBER

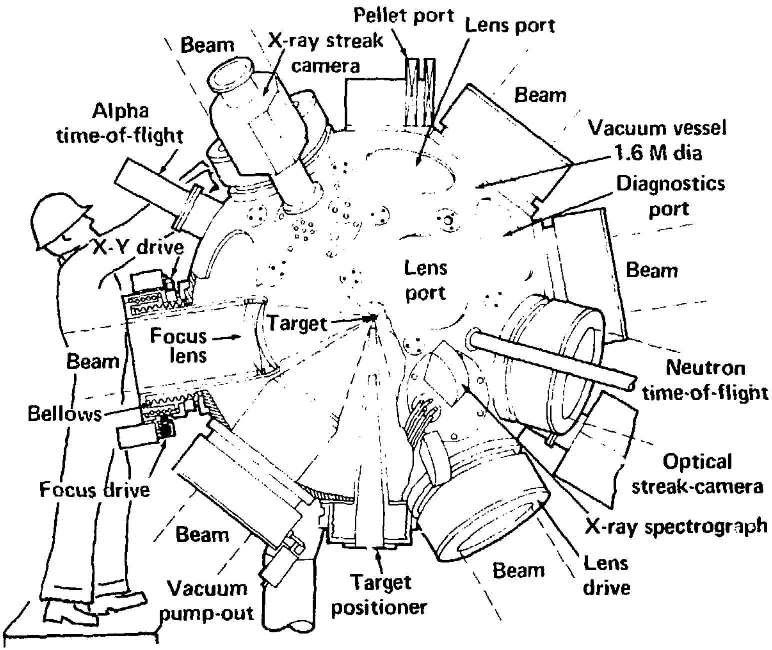

FIG. 2

SHIVA SPACE FRAME

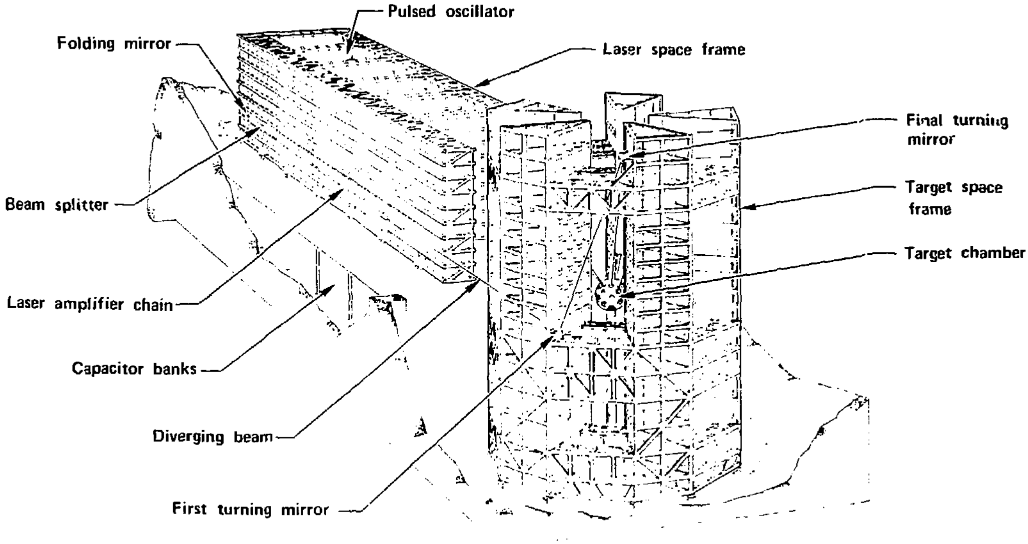

INTENSITY REDUCTION FROM PHASE ABERRATION

$$I/I_0 \approx 1/\left[1 + \frac{\pi (f^{\#})^2 \, P}{(d/D)^2 \, \Delta Z}\right]^2$$

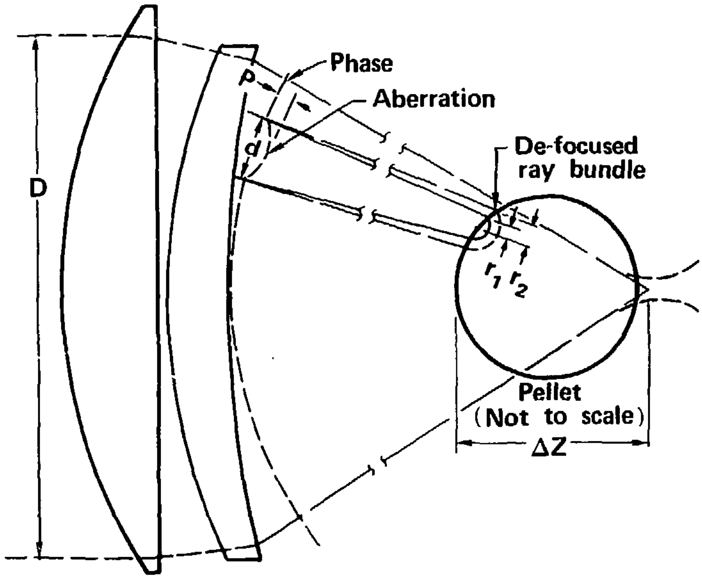

Fig. 3

NEAR FIELD REDUCED INTENSITY FROM PHASE ABERRATION

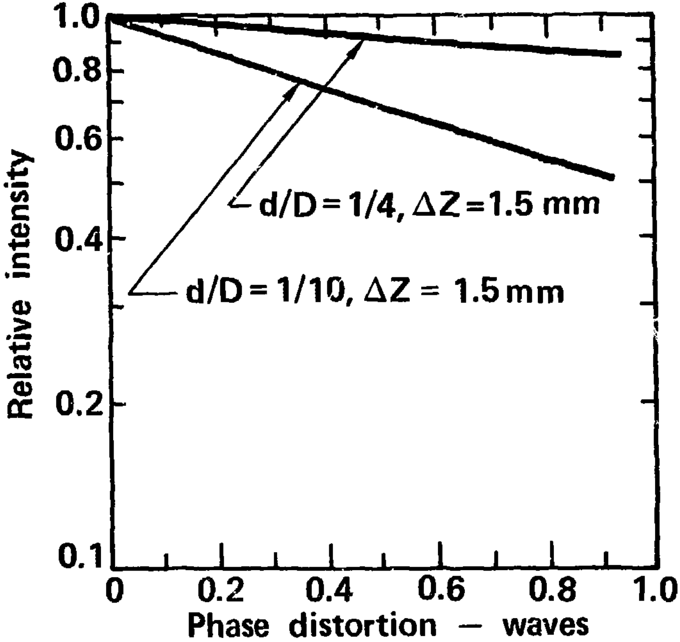

Fig. 4

SHIVA LENS/TARGET GEOMETRY

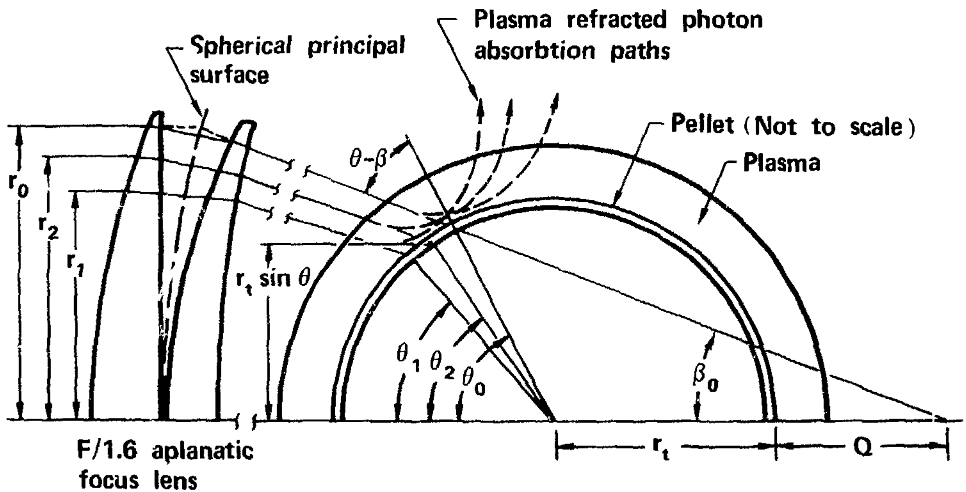

FIG. 5

FIG. 6

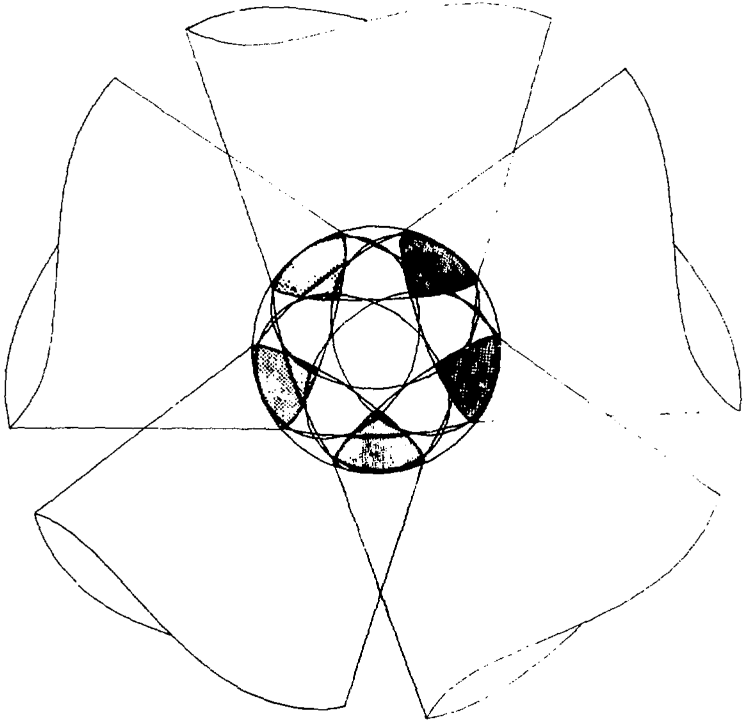

Shiva DT pellet with
20 overlapped focal spots
in icosahedral positions

FIG. 7

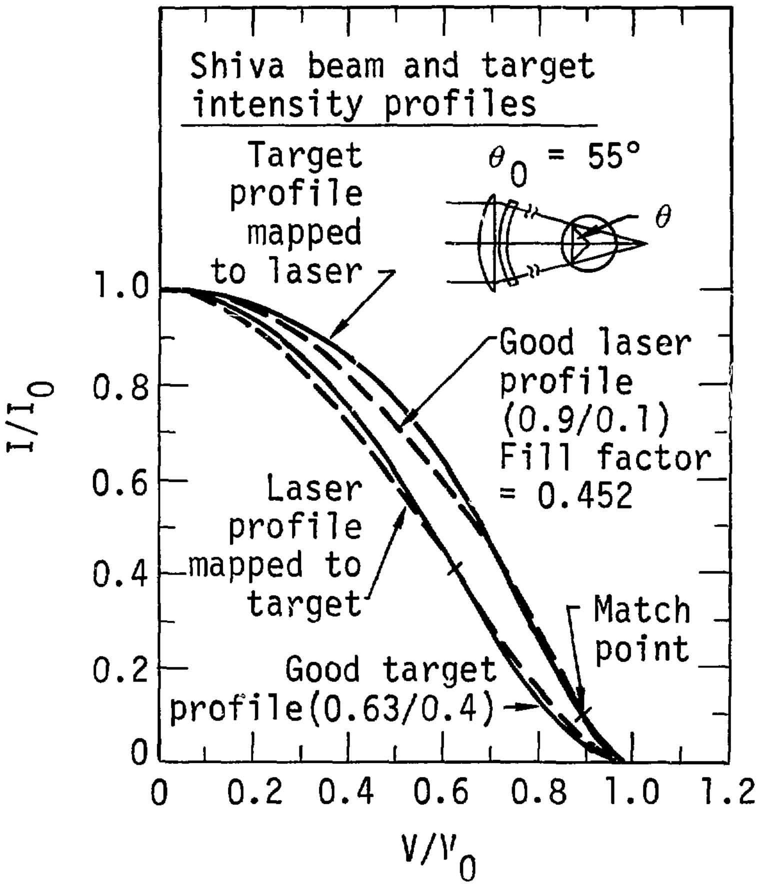

Shiva beam and target intensity profiles
Target profile mapped to laser
θ_0 = 55°
θ
Good laser profile (0.9/0.1) Fill factor = 0.452
Laser profile mapped to target
Match point
Good target profile(0.63/0.4)
1.0
0.8
0.6
0.4
0.2
0
I/I_0
0
0.2
0.4
0.6
0.8
1.0
1.2
V/V_0

CRITICAL CRACK DEPTH, "a", STRESS, AND DEFLECTION IN A GLASS VACUUM-LOADED WINDOW

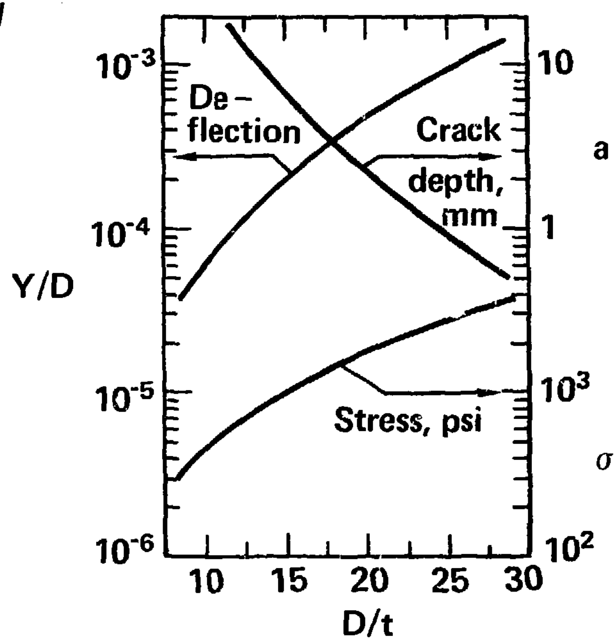

Fig. 8

LENS SURFACE REFLECTIVITY USED IN GHOST FOCUS INTENSITY CALCULATIONS

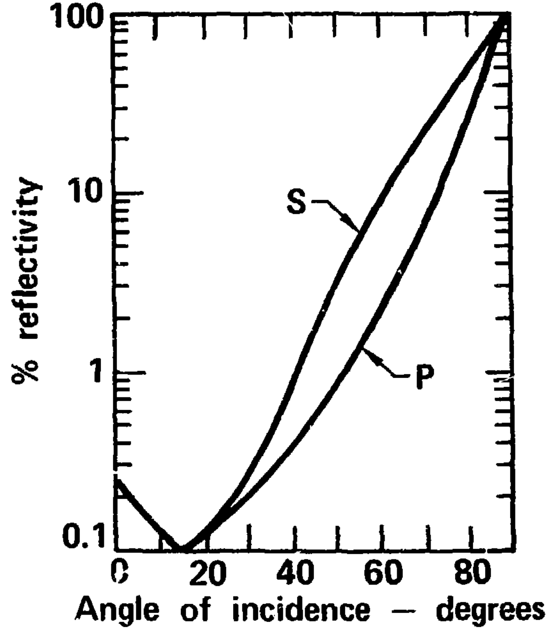

FIG. 9

FIG. 10

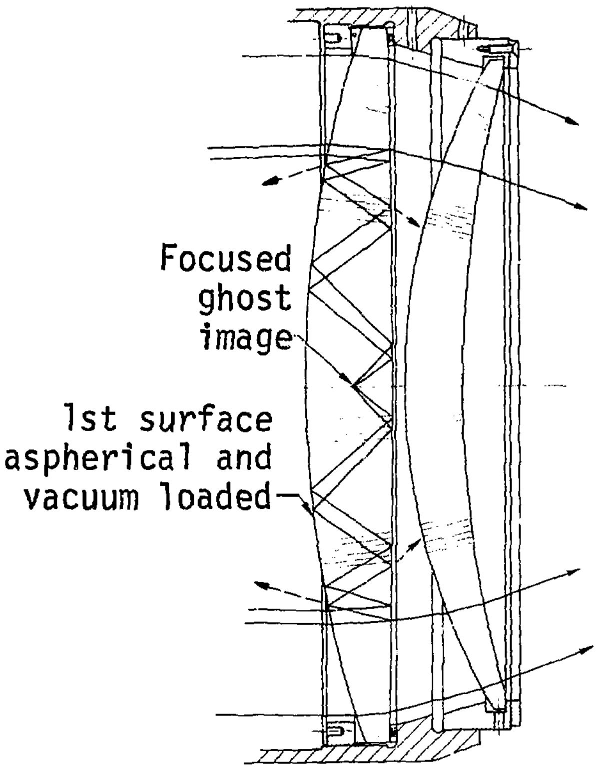

Shiva F/1.6 focus lens 330 mm dia, 465 mm focal length

APPENDIX A

Lens Specification

GENERAL

A. All dimensions are in mm unless otherwise noted.

B. Refer to MEL 74-001247 for clarification of LLL metric policy.

C. Where noted the following specifications apply: MIL-M-13508, MIL-O-13830, MIL-C-675.

D. Unless otherwise specified testing shall be per MEL 75-001271, where applicable.

E. Iron compounds shall not be used for grinding or polishing.

F. Location of surface defects shall be referenced clockwise from the center of the serial number.

G. All inspection data shall be provided by the manufacturer. The inspector shall initial each entry in the inspection record.

H. All specifications apply to the finished lens after cleaning, if cleaning is necessary, over the clear aperture.

I. Seller shall submit his fabrication, testing and inspection plan with the bid. LLL shall approve the plan before fabrication.

STEP 1 - BLANK FABRICATION (LLL WILL SUPPLY BLANKS TO THESE SPECS)

1.1 Material shall be BK-7 or equivalent and visibly free of undissolved metallic inclusions.

1.2 Attenuation coefficient shall be less than .002/cm at 1.06 μm.

1.3 Refractive index homogeneity: variation in refractive index shall not exceed $\pm 1 \times 10^{-6}$ over the clear aperture.

1.4 Birefringence shall not exceed 6 nm/cm.

1.5 Total bubbles, seeds, and inclusion cross section in any 100 cm^3 of glass shall not exceed 0.03 mm^2. Longest dimension of single bubble seed or inclusion shall not exceed 0.2 mm. There shall be no defects in the central 10 mm dia. of the blanks.

1.6 Internal and surface damage threshold shall be greater than 90 GW/cm^2 delivered in 0.1 ns and greater than 30 GW/cm^2 delivered in 1.0 ns at 1.06 μm. LLL may measure damage threshold after receiving blank. Seller shall furnish two witness samples as shown (uncoated) with each blank made from the same melt as the blank.

1.7 Striations shall not be visible in a near field shadowgram or in a Schlieren knife-edge test at 0.6328 μm.

1.8 The LLL serial number indicated on the purchase order must be applied by dental sandblasting or chemical etch with a typed template to each blank and each witness sample. Vibratory or scribe type markings are not acceptable. Any other method must be approved by LLL.

1.9 Inspection documentation: on the inspection report of each blank:

A. Record the attenuation coefficient at 1.06 μm of each melt.

B. Record birefringence at 0.6328 μm of each blank.

C. Record the size and location of all defects in each blank.

D. Record the index of refraction at 1.06 μm and 0.6328 μm of each blank.

E. Provide the near-field striation shadowgram and two photographs of a Schlieren knife edge test with the knife edge rotated 90° at 0.6328 μm of each blank.

F. Record homogeneity and provide interferograms.

STEP 2 - SURFACE FINISHING

2.1 Edge chips shall conform to MIL-O-13830 paragraph 3.7.9.2.

2.2 Deviation of the beam due to centering error shall not exceed 10 arc seconds.

2.3 Single pass peak to valley wavefront distortion of assembly and element 1 alone shall be less than λ/10 with a gradient less than λ/24/cm at 1.06 μm over the clear aperture, tested in the configuration shown on this drawing, or equivalent, with no vacuum load on surface 1. LLL shall approve sellers test configuration before lens fabrication.

2.4 Quality of surfaces 1, 2, 3, 4 shall meet or exceed 40/10 scratches and digs as defined in MIL-O-13830 (over full diameter for surface 2).

2.5 Edges of the lens shall have a fine grind finish equivalent to an A.O. 303 1/2 finish.

2.6 (REF) Surface figure for lens surface 1 for BK7 at 1.06 μm: (REF Refractive index: 1.5701) Surface 1 is an aspheric surface given by the following equation:

$$Z = \frac{CY^2}{1 + (1 - (K + 1)\ C^2Y^2)^{1/2}} + DY^4 + EY^6 + FY^8 + GY^{10}$$

where Z = axial distance from center of surface 1, mm

input beam divergence - 3 mrad full angle

Y = vertical height from axis, mm

C = vertex curvature, mm = 2.36658 E-3

K = conic constant = -0.294377

D = polynomial coefficient, mm^{-3} = -7.01581 E-10

E = polynomial coefficient, mm^{-5} = -2.81118 E-15

F = polynomial coefficient, mm^{-7} = +6.28544 E-21

G = polynomial coefficient, mm^{-9} = -2.48339 E-25

(REF) Best fit radius R_1 to edge (330 dia.): 434.42

(REF) Aspheric deviation max. ∿ 0.23

2.6.1 *Surfaces 2, 3, and 4:* (surfaces 2, 3, and 4 are LLL designed to minimize the intensity of internal ghost focus images).

R_2 = radius of surface 2, mm = -4070.17 ± 40

R_3 = radius of surface 3, mm = 291.545 (REF)

R_4 = radius of surface 4, mm = 461 ± 5

Seller shall design surfaces 1 and 3 to meet the requirements of this drawing, using the specific melt index of refraction at 1.06 µm. Final design figures shall be approved by LLL before lens fabrication.

2.6.2 Surfaces 3 and 4 shall not deviate from true spherical by more than 0.06 µm.

2.7 Inspection documentation: (for coated parts the following documentation requirements apply before and after coating.) On the inspection report of each lens:

A. Record the size of the largest edge chip and the number of chips on each edge.

B. Provide orthogonal polaroid or equal interferograms of wavefront distortion for element 1 and assembly, without vacuum load (4 total).

C. Record measured scratches and digs - size and location.

STEP 3 - COATING FINISHED SURFACES

3.1 Surfaces 1, 2, 3 and 4 shall have a hard dielectric coating applied over the clear aperture. The coating is for enhanced transmission and suppression of ghost reflections. Reflectivity requirements for each surface are:

External Angle of Incidence	Average of P&S Polarization
0°	$\leq$ 0.25%
15°	$\leq$ 0.10%
30°	$\leq$ 0.25%
45°	$\leq$ 0.75%
60°	$\leq$ 1.00%

3.2 Loss due to sum of coating scattering and absorption shall not exceed 0.2%/surface.

3.3 Coating damage threshold shall be greater than 30 gw/cm^2 delivered in 0.1 ns and greater than 10/gw/cm^2 delivered in 1.0 ns measured normal to the 1.064 µm laser beam. A witness sample to be coated with each side of each lens will be provided by LLL for use in LLL tests to assure that the lens will meet or exceed the specified damage threshold. The witness samples shall be marked with the lens serial numbers as per note 1.8. LLL may measure damage threshold (on lens) after receiving finished part.

3.4 Cleaning coated surfaces shall be avoided. However, if it is required, the cleaning method must be approved by LLL, and the witness samples must be cleaned in the same manner.

3.5 Hardness and adherence requirements shall conform to MIL-M-13508 paragraphs 3.8 and 3.9 and MIL-C-675 paragraphs 3.9.2 and 3.9.4.

3.6 Inspection documentation: In the inspection report for each lens:

A. On one surface from each run: Measure P & S reflectivity at four spots 2 mm in diameter approximately 90° apart at 7/10 zone at 0°, 15°, 25°, 45°, 60° angles of incidence, and four other spots 90° apart at 5/10 zone at 15° angle of incidence.

B. On one witness sample from the first run of each series of runs using P polarized 1.064 µm laser light at Brewster's angle: measure precoated transmission of glass, one sided coated transmission of sample, and reflectivity of coating, to determine that scattering and absorption of coating is within normal limits.

C. Record that the hardness and adherence requirements are met on one hardness witness sample per coating run. Actual tests shall not be performed on the lens or the damage test sample.

D. Record whether or not a surface has been cleaned and if so by what method.

E. Record inspection specified in 2.7 A and C for the coated lenses.

STEP 4 - ASSEMBLY

4.1 Assembly and test operation may be required both before and after coating as stipulated on purchase order.

4.2 Assemble in LLL supplied lens cell per Drawing no. AAA 76-104844.

4.3 Provide orthogonal interferograms of assembly wavefront distortion without vacuum demonstrating assembled performance as indicated in paragraph 2.3.

4.4 Provide orthogonal interferograms of assembly wavefront distortion with vacuum load on surface 1 after completion of step 4.3.

4.5 Assembly operation shall not degrade the recorded scratch and dig quality resulting from the previous operation or introduce edge chips in excess of the tolerance.

4.6 After coating, the assembly is to be clean and between the lens region is to be free of dust particles to a class 100 level. Cleaning coated surfaces should be avoided. However, if it is required, the cleaning method must be approved by LLL.

4.7 Inspection documentation

A. Record cleaning methods used for coated glass surfaces (see paragraph 4.6).

B. Record measured scratches and digs - size and location.

C. Supply interferograms per paragraphs 4.3 and 4.4.

D. Provide results of vacuum test (see Drawing AAA 76-104844-00 Note 9).

E. Provide inspection report on between-lens cleanliness of assembly.

STEP 5 - PACKAGING

5.1 Parts shall be cleaned and packaged per LLL MEL 76-001311 "cleaning and packaging procedure for laser optics" or vendor procedure approved by LLL.

5.2 LLL will supply a class 100 shipping box that will properly contain the optical element and its inspection data.

5.3 The individual component or assembly boxes shall be packaged in a suitable secondary box with adequate packing around it to protect it from the shock of commercial handling.

5.4 The outside of the LLL supplied box shall have a stick-on embossed label, with the LLL serial number clearly defined.